

## Modeling of plasma dynamics parameters of magnetoplasma compressor

*N.V. Batrak\**, *N.G. Kopaleishvili*

*Bauman Moscow State Technical University, Moscow, Russia*

*\*svryzhkov@bmstu.ru*

**Abstract.** The prospect of magnetoplasma compressor (MPC) due to their technical and geometrical characteristics are discussed, the formulation of ways to improve their parameters is obtained. Thermal modeling of radiation-magneto plasma dynamic processes of powerful electric discharge sources is presented. The developed mathematical model is based on a nonstationary axisymmetric two dimensional system of equations for viscous one-temperature radiation plasma dynamics. This paper presents results of the numerical calculation.

**Keywords:** magnetoplasma compressor, plasma dynamic mode, magnetogasodynamic rupture, shock wave.

### 1. Introduction

The magnetoplasma compressor (MPC) discharge plasma [1–5] acquires a quasi-stationary structure characteristic of the plasma dynamic mode. The main structural regions of the discharge light-erosion plasma are:

- i) cumulative jet with increased densities and temperatures, bounded by discontinuities (I);
- ii) region (II) of the main electromagnetic acceleration of the dielectric light-emitting plasma, bounded by the system of discontinuities of the and the surface of the face of the MPC;
- iii) dielectric plasma flow through a conical magnetogasodynamic shock wave rupture (III);
- iv) secondary electromagnetic acceleration bounded by the system of discontinuities (IV).

The outer boundary region of the discharge is the characteristic plasma dynamic braking zone of the light-erosion plasma flow on the surrounding gas, consisting of strong gas-dynamic shock waves in the surrounding gas (SWG) and in the plasma flow (SWP) and a contact boundary (CB) separating the shock-compressed gas and plasma region [6, 7].

A significant increase (compared to the transition mode) of velocities in the near-axis region of the light-erosion plasma flow provides an increase in the intensity of shock waves in the region of plasma dynamic braking on the gas: SWG is ionizing SW. Thermal radiation generated by the internal regions of the discharge plasma leads to the radiation wave (RW), which propagates through the undisturbed gas and provides heating of the surrounding gas layers adjacent to the SWG to temperatures of 1–2 kK.

### 2. Plasma dynamic mode

The increase in power  $P_1$ , allocated on plasma load (by increasing  $W_0$  or reducing the duration of the first half-period  $t_1$ ), the amplitude of the discharge current  $J_m$  and a decrease in the density of the surrounding gas  $\rho_0$  determine the increasing role of electromagnetic forces and plasma dynamic effects in the processes of energy and mass exchange and the dynamics of plasma formation. At values  $P_1$ ,  $J_m$  and  $\rho_0$ , corresponding to the area of parameter change  $A_m > 0.8$ , the MPC discharge passes into the plasma dynamic mode with minimal influence of the ohmic mechanism of plasma heating ( $\lambda_R \approx 0.2–0.4$ ) and strengthening of the kinetic energy share of the moving discharge plasma in the total energy balance ( $\lambda_E \approx 0.3–0.4$ ). At the same time, the formation dynamics and structure of the discharge plasma undergoes a number of new qualitative changes [8–13].

Among the features of the configuration of the boundaries of the main structural regions of the light-erosion plasma note the following. The rupture, which is a strong magnetogasdynamic SW rupture and separates the areas of the initial ( $0 < z < z_\Phi$ ) section of the cumulative jet and the main electromagnetic acceleration, has a shape close to the cylindrical. In the vicinity of its terminus, this rupture experiences a characteristic plasma dynamic mode "fracture", intersecting with the conical

magnetogasodynamic rupture. The cumulation region, located behind the point ( $z > z_\Phi$ ), is limited by the tangential discontinuity with a shape (in contrast to the transition mode) close to cylindrical, which is the result of the action of significantly large compressing electromagnetic forces in this region of plasma flow and the interaction of the cumulative jet with the plasma flow. Finally, the process of plasma flow moving in zone III, after the flow passes the conic rupture, is accompanied by the emergence of a gas-dynamic SW rupture, highlighting a zone of repeated electromagnetic acceleration of the plasma flow in region III.

Among the peculiarities of the dynamics of the position of the boundaries of the structural regions of the discharge we can point out a much stronger "pushing away" of the surrounding gas from the end of the MPC by the plasma light-erosion flow than in the transient mode: at the moment of the discharge current maximum the position coordinate of the near-axis SWG zone significantly exceeds the size of the MPC midsection. During the growth phase of the discharge current, the motion of the near-axis SWG occurs with acceleration. For example, in the particular case considered below, by the time  $t = 6.5 \mu\text{s}$ , the velocity of the SWG along the MPC axis is  $\sim 20 \text{ km/s}$  with the average velocity  $D \sim 15 \text{ km/s}$ . The length of the initial section  $z_\Phi$  of the cumulation zone during the first half-period of current increases. At the same time, the propagation velocity is approximately  $D/2 - D/3$ . With time there is a tendency to decrease this velocity to values  $\sim D/3$  (in the area of the discharge current maximum). The lateral boundary of the initial part of the cumulation region moves radially away from the system axis with the speed  $< 1 \text{ km/s}$ .

Processes of formation and plasma structure typical for modes with  $A_m > 0.8$ , let us discuss on the example of MPC with  $C = 750 \mu\text{F}$ ,  $U = 10 \text{ kV}$  in argon with pressure  $10^3 \text{ Pa}$  ( $A_m = 0.85$ ). The time of reaching the discharge current maximum at such MPC parameters is  $t_m = 15 \mu\text{s}$  with the duration of the first half-period  $t_1 = 30 \mu\text{s}$ .

### 3. Numeric simulation results

The calculated spatial distributions of the main thermogasodynamic plasma parameters at the time  $t = 6.61 \mu\text{s}$  for the considered version of the MPC discharge are shown in Fig.1 and Fig.2. As can be seen from the presented results, significant quantitative changes, compared to the transition mode, occurred in the main electromagnetic acceleration zone, the plasma parameters in which determine the plasma parameters in the cumulation zone. In more energetically powerful modes of MPC discharges carried out in less dense gases, the value of the plasma velocity increases significantly in region II. The plasma velocities attainable at the boundaries of region II, equal to the local Alfvén velocities, are values from 10 to 60 km/s.

Modeling is carried out in barrier geometry, i.e. the computational domain is a set of layers. The thickness and properties of substance in the layer can be arbitrarily varied. Charged particles injected into the calculation area can have an arbitrary initial energy (or spectrum) and angular distribution.

Here it should be noted that by the considered moment of time ( $t = 6.5 \mu\text{s}$ ) there is a developed light-erosion evaporation of the central electrode surface (delayed evaporation of the central electrode in this case was  $\sim 3 \mu\text{s}$ ) and, directly on the MPC axis, already formed a dense narrow ( $r < 2 \text{ mm}$ ) jet of metal plasma extending 15 mm in  $z$ -direction. The jet is compressed by the magnetic field of the discharge current and the dynamic pressure of the collapsing flow of dielectric plasma. As a result, a dense ( $0.1 - 0.4 \text{ kg/m}^3$ ) and high-temperature ( $100 - 150 \text{ kK}$ ) nearside region of the cumulative jet is formed in close proximity to the end of the central electrode.

The increase in the velocity (both in the axial and radial directions) of the dielectric plasma in the zone of continuous electromagnetic acceleration II before the rupture as it moves away from the surface of the MPC leads, as in the transient mode, to the intensification of the shockwave rupture as it approaches special point. Since this decreases the dielectric plasma density before the rupture,

the plasma density value of the rupture passed, but increases its  $z$ -component velocity as it moves away from the MPC end. Thus, a less dense (compared to the near-axis zone) peripheral zone of the cumulative jet is formed, whose interaction with the near-axis plasma is one of the main mechanisms of acceleration of the latter.

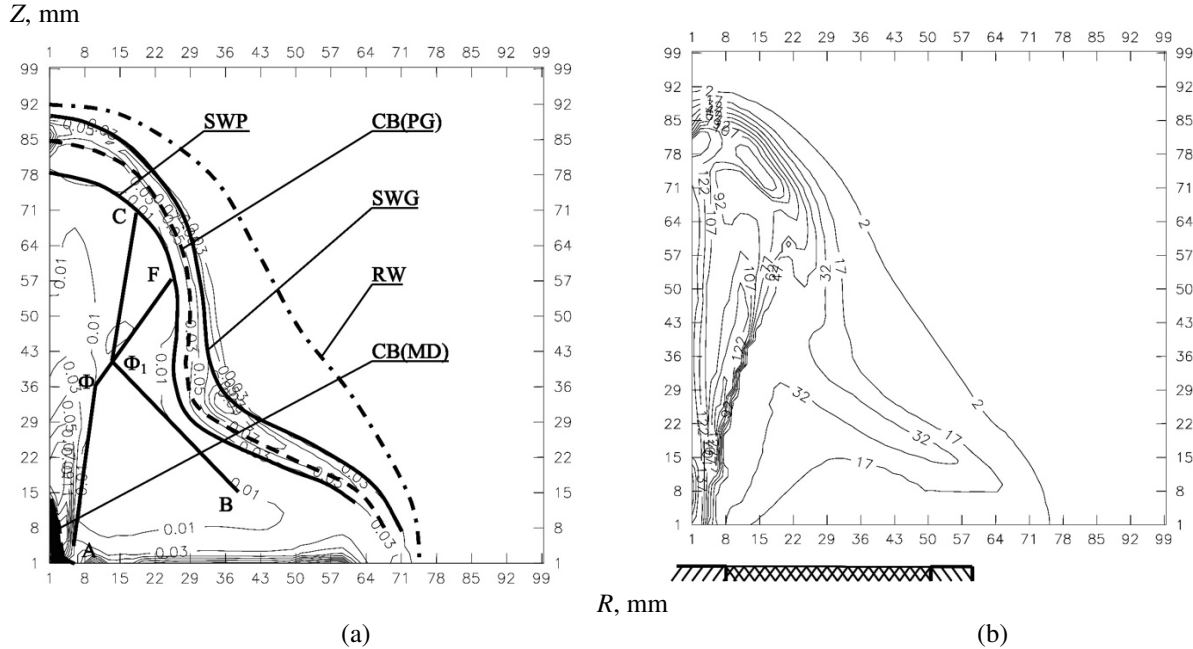


Fig.1. Density level lines [kg/m<sup>3</sup>] (a), temperature [kK] (b) at discharge current  $J = 353$  kA for MPC ( $R_1 = 0.8$  cm,  $R_2 = 5$  cm) with parameters  $C = 750$   $\mu$ F,  $U = 10$  kV in argon with pressure  $10^3$  Pa ( $A_m = 0.85$ ).

Significant is the fact that the high level of dielectric plasma velocities ( $>10$  km/s) in both the axial and radial directions is achieved in the vicinity of the central electrode (near point A) at a small ( $< 0.5$  cm) distance from the dielectric surface i.e., in the zone where the dielectric plasma density is quite high ( $> 0.03$  kg/m<sup>3</sup>). Radial collapse of such dense plasma on the MPC axis leads first to shock wave compression of plasma and then, already in the cumulation zone, subsequent compaction under the action of inertial and electromagnetic forces (compression effect).

The level of the radial velocities and densities of the dielectric plasma in zone II before the rupture is such that the magnetogasodynamic shock wave becomes radiative, approaching the critical SW in its parameters [14]. This manifests itself in the "throwing" of the temperatures of the shock-compressed plasma immediately behind the rupture front, the maximum values of which, in this particular case, are 120–130 kK near point behind the rupture line and behind the rupture line. At the same time, before the indicated ruptures in the plasma of region II, the appearance of a zone of radiative heating to a temperature of 40 kK, characteristic of radiative shock waves is observed.

We should pay attention to the appearance of characteristic for the plasma dynamic mode of the MPC "fracture" (see Fig.1a) in the system of discontinuities limiting the cumulation region. As shown by the calculations (Fig.2b), the absolute values of the plasma velocity monotonically increase with distance from the surface of the MPC face and reach the maximum (equal to the local Alfvén velocities) values in the area (60–70 km/s in this case). At the same time, the angle of slope of the velocity vector to the MPC axis monotonically decreases: the value of the radial component of the flow velocity becomes less than the axial, which leads to a break of the front of the cylindrical SW and the formation of the SW rupture, whose boundary is almost perpendicular to the velocity vector of the advancing plasma flow. Shock wave braking of the dielectric plasma flow with maximum plasma velocities and minimum densities before the rupture causes the maximum

plasma dynamic heating of the plasma: just behind this rupture is formed a localized zone of dielectric plasma with maximum temperature values (120–130 kK in this particular case). It should be noted that the heating of the plasma in this localized zone occurs as a result of the collision in this place of the dielectric plasma flows that have passed to this zone from region III and from the peripheral regions of the cumulation zone. The emergence of such a zone of elevated temperatures can be interpreted as a zone of “secondary” cumulation.

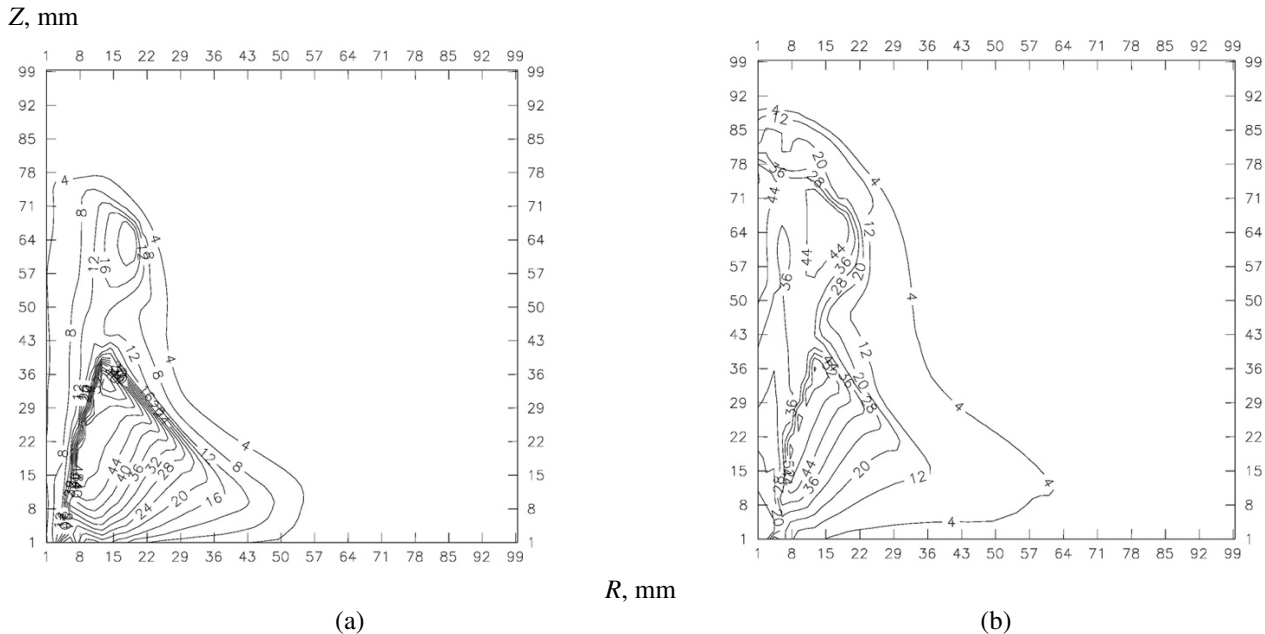


Fig. 2. Alfvén velocity level lines (a), and velocity modulus (b) [km/s] at time  $t = 6.5 \mu\text{s}$  for MPC ( $R_1 = 0.8 \text{ cm}$ ,  $R_2 = 5 \text{ cm}$ ) with parameters  $C = 750 \mu\text{F}$ ,  $U = 10 \text{ kV}$  in argon.

The initial cumulation zone is followed by an area (limited by the surface of the tangential discontinuity), where there is further acceleration of the light-erosion plasma flow of the dielectric. At the same time there is a decrease in the flow density, the value of which just before the area of plasma dynamic braking (i.e., before the SWP) is  $0.03\text{--}0.05 \text{ kg/m}^3$ , i.e. less than the density of the surrounding gas. The boundary of this part of the cumulation region is formed as a result of the dynamic effect of the flow of dielectric plasma moving in zone III, as well as the effect of electromagnetic forces, providing additional axial acceleration of the peripheral plasma layers and limiting the radial expansion of the plasma. The essential role of electromagnetic forces in this part of the cumulation zone is an important feature that is characteristic only for the plasma dynamic mode of the MPC discharge ( $A_m > 0.8$ ). The reason is the “deep” (up to the external SWG) penetration of the discharge current through the high-temperature plasma of the cumulation zone. A noticeable part ( $\geq 20\text{--}30\%$ ) of the current flows through the plasma regions outside the areas of the initial cumulation zone and zone II of the main electromagnetic acceleration. This fact is clearly confirmed (Fig. 2a) by the spatial distribution of the Alfvén velocities, by the magnitude of which we can distinguish the discharge region, where the repeated electromagnetic acceleration of the dielectric plasma takes place. As a result of this effect, the peripheral layers of the dielectric plasma in the cumulative zone are accelerated to the velocities 40–50 km/s (Fig. 2b).

An important distinguishing feature of the plasma dynamic mode is the complication of the structure of region III, formed as a result of the dielectric plasma flow passing a conical rupture. On the magnetogasdynamic shock wave, the plasma flow velocity decreases its normal to the rupture line component, which leads to the flow rotation and insignificant heating of the plasma in region

III. The plasma flux moving toward the axis forms an internal conic SW fracture in area III, on which the flux turns from the MPC axis. The interaction of this dielectric plasma flow with the plasma flow formed in the cumulation region leads to the formation of a tangential rupture, which is the boundary separating the cumulation region I and region III. In the second part of the region III, bounded by the discontinuities, as a result of the action of electromagnetic (this zone is in the region of repeated electromagnetic acceleration) and gas-dynamic forces occurs a significant acceleration to speeds 40–45 km/s and turning plasma flow.

#### 4. Conclusion

As a result of the described complex of magnetogasdynamic processes, a spatially inhomogeneous flux of light-erosive dielectric plasma is formed in the internal region of the discharge. The heterogeneity of parameters of this flux leads to various effects of its plasma dynamic inhibition on the gas surrounding the discharge with formation of a characteristic structure: the SW in plasma (SWP), the contact boundary CB and the shock wave in gas (SWG). The rarefied ( $\rho_{pl} < \rho_0$ ) cumulative flow, moving in this case with the velocity  $u_{p0} \sim 50$  km/s, is braked on the gas in the "effective braking" mode [15, 16], in which there is a significant heating of the shock-compressed light erosive plasma to a temperature of 140–200 kK behind the  $Cz_T$  front. In this case, in the oncoming light-erosion plasma flow is formed by a strong SWP moving along the flow. The axial part, which forms a strong SWG, moves with average velocity  $D \sim 15$  km/s. A shock wave of such intensity provides 10-fold densification of the gas and heating it to temperatures 30–40 kK. SWG with the above parameters is itself a powerful source of thermal radiation. The plasma flux in the second part of zone III with velocity  $u_{p0} \sim 40$ –45 km/s and lower density ( $\rho_{pl0} < 0.1\rho_0$ ) is also braked on the gas barrier in the mode of "effective" braking with heating the shock-retarded plasma (behind the break line CF) to the temperature 100 kK.

#### 5. References

- [1] Shanenkova Y., Sivkov A., Rahmatullin I., Tsimmerman A., Ivashutenko A., Osokina L., *Proc. of 7<sup>th</sup> International Congress on Energy Fluxes and Radiation Effects (EFRE 2020)*, Tomsk, Russia, 1324, 9242032, 2020; doi: 10.1109/EFRE47760.2020.9242032
- [2] Pavlov A., Protasov Y., Telekh V., Tshepanuk T., *J. Phys.: Conf. Ser.*, **830**, 012062, 2017; doi: 10.1088/1742-6596/830/1/012062
- [3] Kuzenov V.V., Ryzhkov S.V., Varaksin A.Y., *Applied Sciences*, **12**, 3610, 2022; doi: 10.3390/app12073610
- [4] Nosov K.V., Pavlov A.V., Protasov Y.Y., Telekh V.D., Tshepanuk T.S., *J. Phys.: Conf. Ser.*, **1115**, 032011, 2018; doi: 10.1088/1742-6596/1115/3/032011
- [5] Kuzenov V.V., Ryzhkov S.V., Frolko P.A., *J. Phys.: Conf. Ser.*, **830**, 012049, 2017; doi: 10.1088/1742-6596/830/1/012049
- [6] Kozlov A.N., *Contrib. Plasma Phys.*, **60**, e201900174, 2020; doi: 10.1002/ctpp.201900174
- [7] Shanenkov I.I., Pak A.Ya., Sivkov A.A., Shanenkova Yu.L., *MATEC Web of Conferences*, **19**, 01030, 2014; doi: 10.1051/mateconf/20141901030
- [8] Kuzenov V.V., Ryzhkov S.V., *Computational Thermal Sciences*, **13**, 45, 2021; doi: 10.1615/ComputThermalScien.2020034742
- [9] Kuzenov V.V., Ryzhkov S.V., *Applied Physics*, **3**, 26, 2014; EID: 2-s2.0-84916912008
- [10] Kuzenov V.V., Ryzhkov S.V., Starostin A.V., *Russian Journal of Nonlinear Dynamics*, **16**, 325, 2020; doi: 10.20537/nd200207
- [11] Kuzenov V.V., Ryzhkov S.V., *Physics of Plasmas*, **26**, 092704, 2019; doi: 10.1063/1.5109830
- [12] Kuzenov V.V., Ryzhkov S.V., *Journal of Enhanced Heat Transfer*, **25** (2), 181, 2018; doi: 10.1615/JEnhHeatTransf.2018026947

- [13] Kuzenov V.V., Ryzhkov S.V., *Symmetry*, **13**(6), 927, 2021; doi: 10.3390/sym13060927
- [14] Zel'dovich Ya.B., Raizer Yu.P., *Physics of shock waves and high-temperature hydrodynamic phenomena*. (Moscow: Nauka, 1966).
- [15] Kamrukov A.S., Kozlov N.P., Protasov Yu.S., Shashkovskii S.G., *High Temp.* **27**, 141, 1989;
- [16] Grishin Yu.M., Kozlov N.P., Kuzenov V.V., *Computational Mathematics and Mathematical Physics* **34**, 1489, 1994;